Journal of Physiology (1992), **447**, *pp.* 309–327
With 12 figures
Printed in Great Britain

PROTON-INDUCED SODIUM CURRENT IN FRESHLY DISSOCIATED HYPOTHALAMIC NEURONES OF THE RAT

BY SHINYA UENO, TOSHIO NAKAYE AND NORIO AKAIKE

From the Department of Neurophysiology, Tohoku University School of Medicine, Sendai 980, Japan

(*Received 30 October 1990*)

SUMMARY

1. The proton-gated current was investigated in freshly dissociated ventromedial hypothalamic (VMH) neurones from 4-week-old Wistar rats, under whole-cell configuration by the use of the 'concentration-clamp' technique which combines intracellular perfusion with the rapid exchange of external solution within 1–2 ms under a single-electrode voltage-clamp condition.

2. The proton-gated current increased in a sigmoidal fashion as extracellular pH (pH_o) decreased. In external solution containing 2 mM-Ca^{2+}, the threshold of current activation was at pH_o 6·5, and the maximum response appeared at pH_o 4·1–3·9. The dissociation constant (K_d) and Hill coefficient were $10^{-4.9}$ M ($pH_o = 4.9$) and 1·5 respectively.

3. Decreasing extracellular Na^+ concentration reduced the proton-gated current. The current reversed direction at the Na^+ equilibrium potential (E_{Na}), indicating that it was carried by Na^+.

4. The activation phase kinetics of proton-induced current was single exponential. The time constant of activation (τ_a) did not have a potential dependence but decreased slightly by decreasing pH_o. The inactivation phase kinetics was two-exponential. The time constant of inactivation (τ_i) consisted of fast and slow components (τ_{if} and τ_{is}, respectively). Like τ_a, both τ_{if} and τ_{is} did not have any potential dependence, but they slightly increased with decreasing pH_o.

5. The steady-state inactivation curve, constructed by decreasing pH_o from various conditioning pH_os to 4·1, revealed that the proton-induced current had a half-maximum inactivation at pH_o 6·2.

6. The proton-induced current was suppressed as the extracellular Ca^{2+} concentration ($[Ca^{2+}]_o$) increased from almost free (0·01 mM) to 80 mM. Increasing $[Ca^{2+}]_o$ increased τ_a, but slightly decreased both τ_{if} and τ_{is}.

7. Recovery of proton-induced current from complete inactivation of proton-induced current depended on the degree of pH_o change. A bigger change in pH_o induced faster recovery than a smaller change.

8. External divalent cations inhibited the proton-induced current, and the inhibitory potency was in the order of $Mn^{2+} > Co^{2+} > Ca^{2+} > Sr^{2+} > Ba^{2+} > Mg^{2+}$.

9. Tetrodotoxin (TTX) at relatively low concentration ($< 10^{-7}$ M) did not inhibit the peak amplitude of the proton-induced current, but at a higher concentration

(10^{-6} M) it slightly inhibited the peak amplitude of the current and accelerated the inactivation process. Scorpion toxin markedly increased the peak amplitude of the proton-induced current and prolonged the inactivation phase. The τ_{is} was also increased by scorpion toxin in a concentration-dependent manner. Veratridine had no effect on the proton-induced current.

10. The membrane properties of the proton-operated channel were similar to those of the voltage-gated Na^+ channel rather than the Ca^{2+} channel.

INTRODUCTION

The extracellular hydrogen concentration ($[H^+]_o$) is regulated within a narrow range in the physiological state. In the CNS an increase in $[H^+]_o$ occurs in pathological states such as ischaemia, seizure, trauma, etc. (Cragg, Patterson & Purves, 1977; Kraig, Ferreira-Filho & Nicholson, 1983). An increase in $[H^+]_o$ affects the membrane surface charge, receptor proteins and voltage-gated channel proteins (Hille, 1968; Campbell & Hille, 1976; Campbell, 1982; Begenisich & Danko, 1983). The excitability of most neurones is depressed by an increase in $[H^+]_o$ (Takahashi & Ogawa, 1987; Balestrino & Somjen, 1988; Jarolimek, Misgeld & Lux, 1989). However, a rapid increase in $[H^+]_o$ has been reported to elicit a transient Na^+ current in rat trigeminal neurones (Krishtal & Pidoplichko, 1981*a*, *b*), rat tectal neurones (Grantyn & Lux, 1988), chick dorsal root ganglion (DRG) cells (Konnerth, Lux & Morad, 1987), frog DRG cells (Akaike, Krishtal & Maruyama, 1990), and frog heart parasympathetic neurones (Kim, Tateishi & Akaike, 1990). Recently, we used the extremely rapid concentration-jump technique (termed concentration-clamp technique) in freshly dissociated mammalian CNS neurones (Akaike, Kostyuk & Osipchuk, 1989) and successfully analysed the kinetics and pharmacological properties of voltage-dependent Na^+ and Ca^{2+} currents (Wakamori, Kaneda, Oyama & Akaike, 1989; Takahashi & Akaike, 1990) and drug-gated currents (Nakagawa, Shirasaki, Tateishi, Murase & Akaike, 1990). In the present study we investigated the electrical and pharmacological properties of the proton-induced current in rat dissociated ventromedial hypothalamic neurones by using the concentration-clamp technique under single-electrode voltage-clamp conditions.

METHODS

Preparation

Ventromedial hypothalamic (VMH) neurones were acutely dissociated from 4-week-old Wistar rats according to the procedures published elsewhere (Akaike *et al.* 1989; Shirasaki, Nakagawa, Wakamori, Tateishi, Fukuda, Murase & Akaike, 1990). Briefly, rats were decapitated under ether anaesthesia, and their brains were removed. The brain was sectioned in the coronal plane using a microslicer (Dosaka DTK-1000, Osaka, Japan). The slices containing the VMH region were treated with Tyrode solution containing 1000 U/ml dispase for 60 min at 31 °C. In some experiments, the slices were treated with pronase (0·25 mg/ml) for 15 min in Tyrode solution at 31 °C, and then with thermolysin (0·25 mg/ml) for another 15 min (Gray & Johnston, 1985). After these enzyme treatments, the slices were washed with the Ca^{2+}-free Tyrode solution containing ethyleneglycol-bis-(β-aminoethylether)-*N,N,N',N'*-tetraacetic acid (EGTA, 2·4 mM). Subsequently, the VMH region of the slices was punched out and mechanically dissociated by gentle pipetting in a plastic dish (Corning, 35 mm). Dissociated VMH neurones were kept in Tyrode solution bubbled with 100% O_2 at room temperature (20–23 °C). These cells remained viable for electrophysiological

studies for up to 6 h after dissociation. The dissociated neurones having a diameter of 10–15 μm and input resistance of more than 2 GΩ (2·7 ± 0·3 GΩ, mean ± S.D. in 30 neurones) were used.

Electrical measurements

The suction-pipette technique was applied to dissociated VMH neurones (Akaike *et al.* 1989). The electrodes were positioned close to the neurones by a water-driven micromanipulator (Narishige, MW-3, Tokyo, Japan) under the visual guidance of a microscope. Recording electrodes for the suction-pipette technique were pulled on a two-stage puller (Narishige, PB-7) and fire-polished on a microforge (Narishige, MF-83). Dissociated neurones were sucked to a recording electrode having a tip interior diameter of about 1 μm and resistance ranging from 2 to 5 MΩ. The membrane patch, aspirated into the recording electrode, was ruptured by negative pressure (-30 cmH_2O). Thereafter, the intracellular ionic composition was exchanged with that of pipette-filling solution. Transmembrane currents were recorded using a patch-clamp amplifier (Nihon Kohden, CEZ-2300). Both current and voltage were simultaneously monitored on a storage oscilloscope (Tektronix, 1135) and stored on FM tape (TEAC, MR-30) for off-line computer analysis using pCLAMP software (Axon Instruments).

Rapid application method of external solution

An extremely rapid concentration-jump termed 'concentration-clamp technique' was used (Akaike, Inoue & Krishtal, 1986). Briefly, the cell-attached tip of the recording electrode was inserted into a polyethylene tube through a circular hole of approximately 500 μm in diameter. The lower end of this tube is submerged to the desired external solution contained in plastic dishes on a turntable. Negative pressure (-35 cmH_2O) applied to the upper end of the polyethylene tube was controlled by an electromagnetic valve driven by 24 V direct current. The power supply was switched on for the desired durations by a pulse generator (Nihon Kohden, SEN-7103). The solution around a dissociated VMH neurone was completely changed within 1–2 ms.

Solutions

The composition of the control external solution was (in mM): 150 NaCl, 5 KCl, 2 $CaCl_2$, 1 $MgCl_2$, 10 glucose, and 10 *N*-2-hydroxyethylpiperazine -*N'*-2-ethanesulphonic acid (HEPES). When the external Na^+ concentration was varied, NaCl was substituted for equimolar choline chloride. The pH of the external solutions ranging from 8·0 to 3·7 was adjusted to the respective values by adding either *N*-methyl-D-glucamine (NMG) or HCl (less than 2 mM at maximum) just before use and confirmed after the experiment. The buffering capacity of HEPES may be insufficient in the lower pH range. However, it was not a key factor in the experiments (cf. Results). Rapid and constant application of solution by the concentration-clamp technique maintained a constant pH around the cell membrane. The composition of the internal solution was (in mM): 100 *N*-methyl-D-glucamine fluoride (NMG-F), 30 NaCl, 20 tetraethylammonium chloride (TEA-Cl), and 10 HEPES. The pH of the internal solution was adjusted to 7·2 by adding an appropriate amount of tris(hydroxymethyl)aminomethane (Tris base).

Drugs

Drugs used in the experiments were tetrodotoxin (TTX; Sankyo), pronase (Hoechst), thermolysin, EGTA, Tris base, 2-(*N*-morpholino)ethanesulphonic acid (MES), and scorpion toxin (*Leiurus quinquestriatus*; all Sigma), HEPES (Dojin, Kumamoto, Japan), *N*-methyl-D-glucamine (NMG; Tokyo Kasei), and veratridine (Aldrich). They were dissolved in the test solutions just before use. All experiments were carried out at room temperature (20–23 °C). Values are expressed as means ± standard error of the mean (S.E.M.), and their significance was tested by Student's *t* test.

RESULTS

Proton-induced inward current

A rapid decrease in pH_o from a conditioning pH_o of 8·0 to various values was made in dissociated VMH neurones, at a holding potential (V_H) of -80 mV, by the use of a concentration-clamp technique. The threshold pH_o to elicit a proton-induced current

in an external solution containing 2 mM-Ca^{2+} was around 6·0. The amplitude of proton-induced current increased in a sigmoidal manner as the test pH_o decreased to 3·7 by adding HCl. No further increase in the amplitude of proton-induced current was observed at test pH_o less than 4·0. Figure 1*B* shows the relationship between

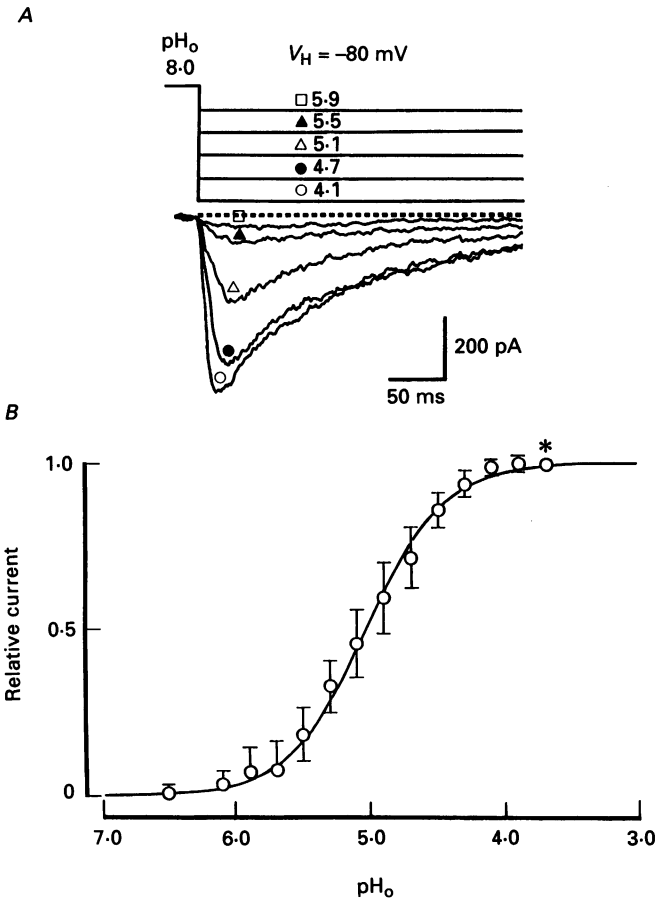

Fig. 1. The pH_o dependence of the proton-induced current in a VMH neurone. *A*, actual current traces evoked by the step decrease of pH_o from a conditioning pH_o of 8·0 at V_H −80 mV. The numbers show the pH_o value of applied test solutions. All external solutions contained 2 mM-Ca^{2+}. *B*, proton-induced currents as a function of pH_o. All proton-induced currents were normalized with respect to the peak response induced by a sudden decrease of pH_o from pH_o 8·0 to 3·7 (*). A continuous line was fitted to experimental data using an equation derived from a concentration–response relation: $(I_{max}-I)/I_{max} = 1/(1+(K/A)^N)$, where K is dissociation constant, A is concentration of H^+ and N is Hill coefficient. The values used to fit the curve were $K = 10^{-4.9}$ M ($pH_o = 4.9$) and $N = 1.5$. Each point is the mean ± S.E.M. of six neurones.

pH_o and proton-induced current, where all proton responses were normalized to the maximum response elicited by a test pH_o at 3·7 (see symbol *). The experimental data fitted well to a theoretical curve with a Hill coefficient of 1·5 and K_d of $10^{-4.9}$ M. The half-maximum activation in the sigmoidal curve was at pH_o 4·9. Similar results were

obtained when the conditioning pH_o was 7·4. Therefore, the following experiments were performed on neurones perfused with an external solution of pH_o 7·4 unless otherwise stated.

Proton-induced currents were affected by the conditioning pH_o. Decreasing the conditioning pH_o reduced the amplitude of proton-induced current (Fig. 2*A*).

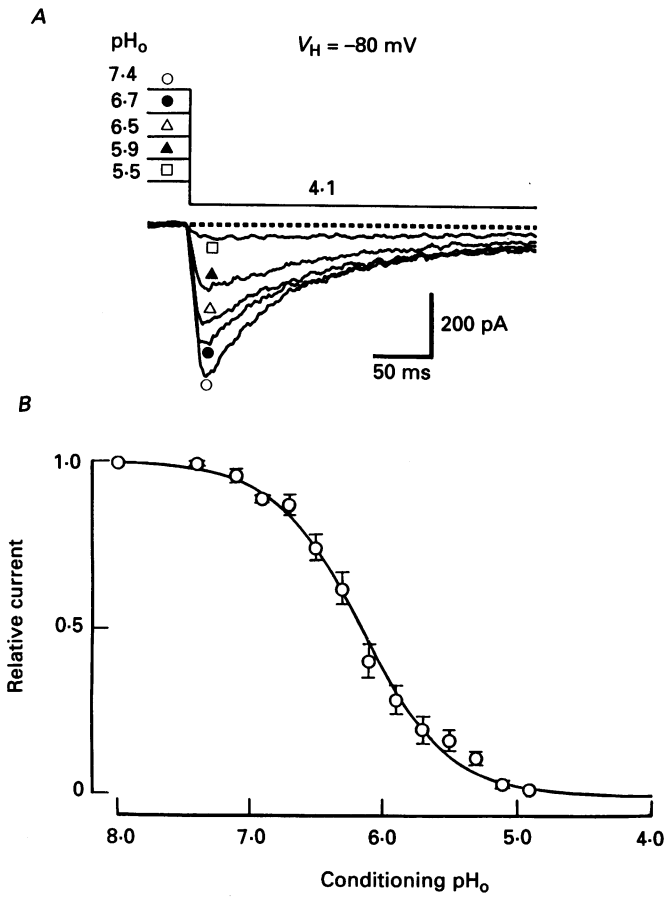

Fig. 2. Conditioning pH_o dependence of the proton-induced inward current. *A*, currents were evoked by step decrease of pH_o from various conditioning pH_os to a constant pH_o of 4·1 at V_H −80 mV. *B*, all proton-induced responses obtained at various conditioning pH_os were normalized to the peak amplitude of current induced by decreasing pH_o from 7·4 to 4·1. Abscissa shows conditioning pH_o. Each point is the mean of six neurones. Vertical bars show ± S.E.M.

Results are summarized in Fig. 2*B* The inhibition curve, which reflects the steady-state inactivation of the proton-induced current, was steep in the conditioning pH_o range of 6·5–5·5. The half-maximum inactivation of the current occurred at a conditioning pH_o of 6·2. The inactivation curve could be fitted assuming a first-order reaction.

In the present experiments, we used test solutions having pH_o less than 4·5. In such low pH solutions HEPES or MES are insufficient as buffer. Hence we tested the

activation and inactivation of proton-induced current in the presence and absence of buffers. Figure 3 shows the activation and inactivation curves of proton-induced current with buffered or unbuffered test solution. HCl was used for low pH adjustment. As shown in Fig. 3*A* and *B* there were no shifts in either the activation or inactivation curves with or without the buffer, respectively.

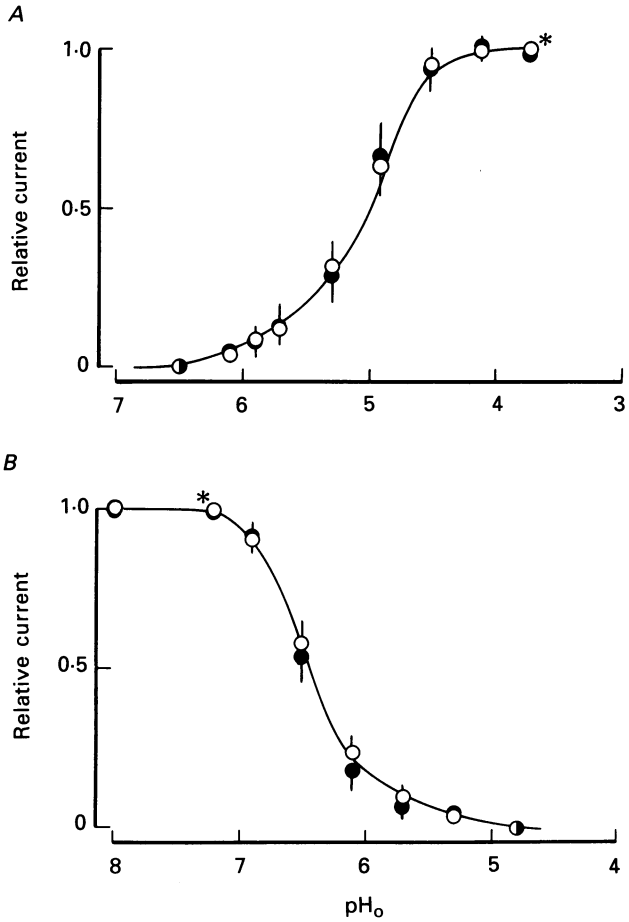

Fig. 3. The activation and inactivation curves of proton-induced current with or without buffers: ○, test solutions with HEPES or MES buffer; ●, without buffer. *A*, proton-induced currents were elicited by the step decrease of pH_o from a conditioning pH_o of 8·0 to various values at V_H −80 mV. All external solutions contained 2 mM-Ca^{2+}. All proton-induced currents were normalized with respect to the peak response (*) elicited by a rapid decrease of pH_o from 8·0 to 3·7 in test solution buffered with 10 mM-HEPES or MES. Continuous lines were drawn theoretically using a half-maximum activation pH_o of 5·1 and the Hill coefficient = 1·5. Each point is the mean ± S.E.M. of six neurones. *B*, currents were evoked by step decrease of pH_o from various conditioning pH_os to a constant pH_o of 4·1 at V_H −80 mV. All proton-induced responses were normalized to the peak amplitude of current (*) induced by decreasing pH_o from 7·4 to 4·1 in 10 mM-HEPES or MES buffer solutions. Each point is the mean ± S.E.M. of six neurones.

The activation phase of the proton-induced current could be described by a single exponent (Fig. 4*A*). Decreasing test pH_o reduced the time constant of activation (τ_a) (Fig. 5*A*). On the other hand, the time constant of the inactivation process (τ_i) consisted of two exponential components, fast and slow (τ_{if} and τ_{is}, respectively)

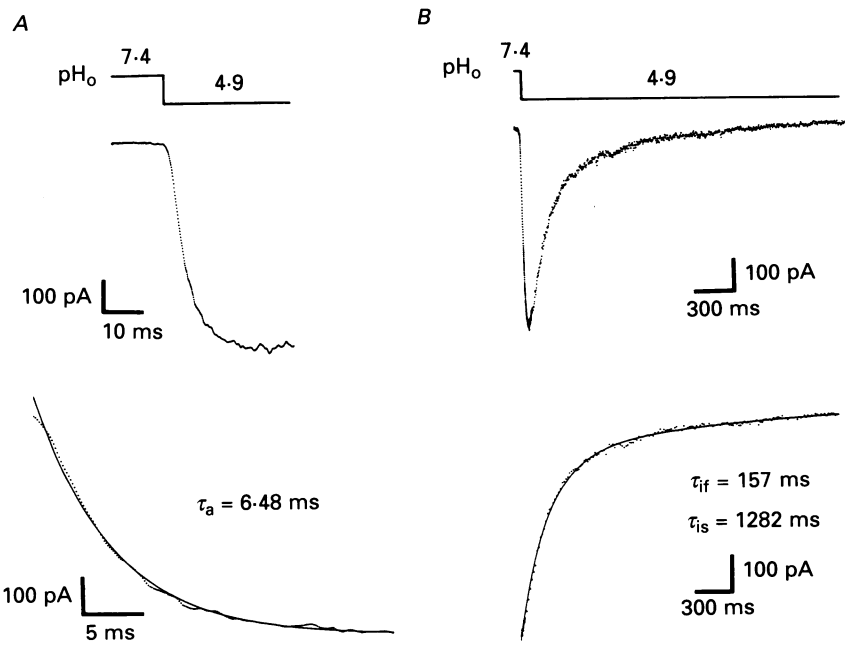

Fig. 4. Activation and inactivation kinetics of the proton-induced current. Current was elicited by decreasing pH_o from 7·4 to 4·9 at V_H −80 mV. *A*, time constant of activation. (τ_a). Calculated fitted curve and data points shown in lower panel. Fit parameter was τ_a = 6·48 ms. *B*, time constants of inactivation. Calculated fitted curve and data points shown in lower panel. Fit parameters were τ_{if} = 157 ms and τ_{is} = 1282 ms.

(Fig. 4*B*). The τ_{is} was about 10 times larger than τ_{if} at all test pH_os examined. Both τ_{if} and τ_{is} slightly increased at lower pH_o (Fig. 5*B*). None of τ_a, τ_{if} or τ_{is} showed any potential dependence when the responses induced by a pH_o change from 7·4 (conditioning pH) to 4·9 were tested at V_H between −100 and +30 mV (Fig. 6).

Recovery from the inactivation of proton-induced currents

The protocol for the step change in pH_o is shown in the upper panel of Fig. 7*A*. The proton-induced current was completely inactivated within 30 s after the application of an acidified solution. Therefore, the recovery process of proton response from the complete inactivation was studied by making a 30 s change in pH_o from conditioning pH_os of 7·4, 6·9, 6·5 and 6·1 to pH 4·5 (V_H = −80 mV). The pH_o was then stepped back to the appropriate conditioning pH for various intervals (Δt) and the response to pH_o 4·3 re-tested. Figure 7*A* (lower panel, results from a single cell) shows that the recovery process from the inactivation greatly depends on the conditioning pH_o. The recovery became much slower at lower conditioning pH_o. This

result indicates that the proton-gated channel of parasympathetic neurones responds to the increase of $[H^+]$ in a manner similar to that in which the voltage-gated channel responds to depolarization. Figure 7*B* shows the recovery time course of proton-induced current at a conditioning pH_o of 6·5 obtained from four cells; 80% recovery to the control took about 10 s.

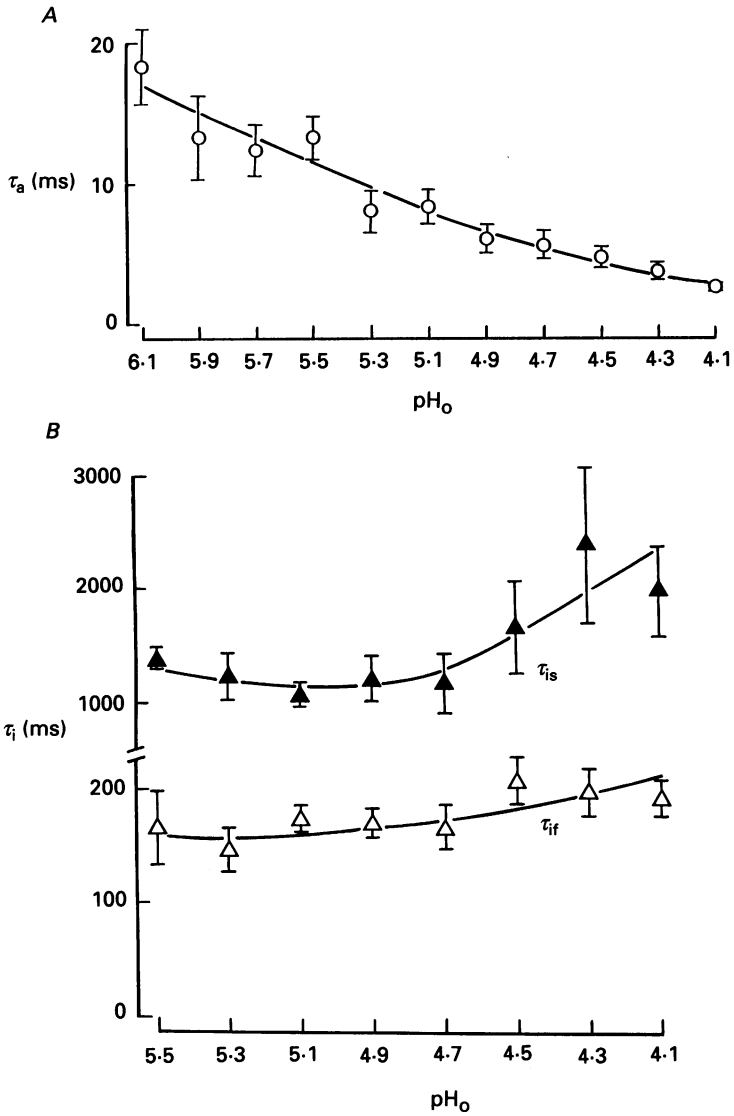

Fig. 5. Effects of pH_o on time constants of activation and inactivation phases of proton-induced currents. Conditioning pH_o was 7·4 at V_H −80 mV. *A*, relationship between time constant of activation (τ_a) and pH_o. Each point is the mean of five to six neurones. Vertical bars indicate ± S.E.M. *B*, relationship between time constants of inactivation (τ_{is} and τ_{if}) and pH_o. Both τ_{if} and τ_{is} slightly increased with decreasing pH_o. This tendency was apparent around pH_o 4·0. Each point is the mean of five to six neurones. Vertical bars indicate ± S.E.M.

Ion selectivity of proton-induced currents

The current–voltage (*I–V*) relationship for the proton-induced currents revealed a reversal potential between +30 and +40 mV (Fig. 8 inset). In these experiments, neurones were perfused with intra- and extracellular solutions containing 150 and

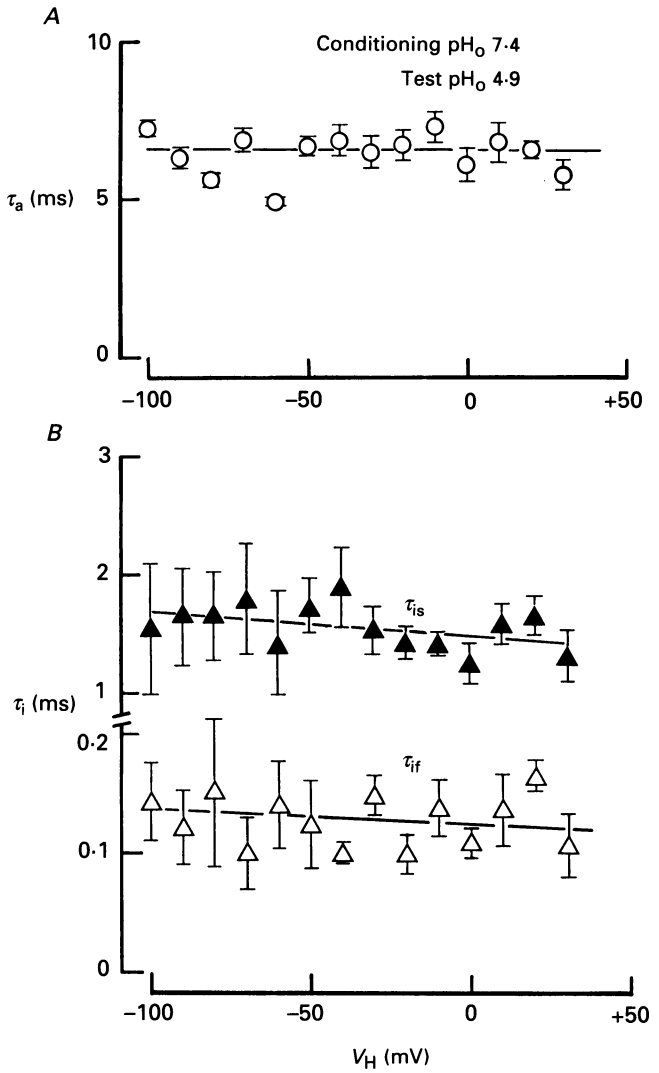

Fig. 6. Effects of V_H on τ_a, τ_{if} and τ_{is} of proton-induced currents. The pH$_o$ was decreased from 7·4 to 4·9. *A*, relationship between τ_a and V_H. The τ_a remained stable in spite of a change in V_H from −100 to +30 mV. Each point is the mean of six neurones. *B*, relationship between τ_{if} or τ_{is} and V_H. The τ_{if} and τ_{is} showed no voltage dependence at V_H ranging between −100 and +30 mV. Each point is the mean of six neurones. Bars are ±S.E.M.

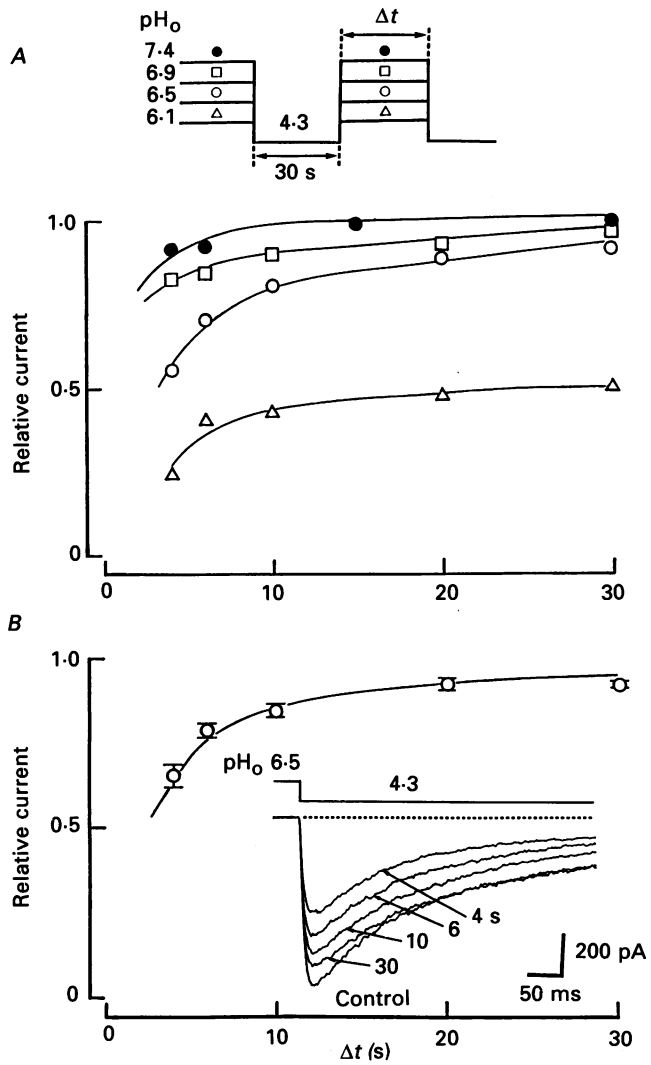

Fig. 7. Recovery from the complete inactivation of proton-induced current. *A*, all recordings were obtained from the same neurone. Upper panel shows the protocol of step changes in pH_o. Each control current was evoked by a first step decrease of pH_o from each conditioning pH_o to 4·3 at V_H −80 mV. Δt indicates a recovery interval between the end of the first application of acidified solution for 30 s and re-application of the same acidified test solution. Lower panel shows the relative proton responses under various conditioning pH_os against recovery interval (Δt in seconds). *B*, the protocol of step changes in pH_o is similar. The control current was evoked by a first step decrease of pH_o from 6·5 to 4·3 at V_H −80 mV. Relative proton responses against recovery interval (Δt in seconds). Each point is the mean of four neurones. Inset shows superimposed actual traces of proton-induced inward currents in the same neurone, evoked by a step reduction of pH_o from 6·5 to 4·3 at V_H −80 mV. The largest current is the control, and the numbers corresponding to the current traces represent the interval period (Δt in seconds) between the end of the first application of acidified solution for 30 s and the re-application of the same acidified test solution.

30 mM-Na^+, respectively. K^+ in both solutions was replaced with equimolar NMG^+. The measured reversal potential (E_{proton} = +39 mV) coincided with the Na^+ equilibrium potential (E_{Na} = +38·5 mV), predicted from the Nernst equation with known intra- and extracellular Na^+ activities (a^i_{Na}, a^o_{Na}). Figure 9 shows the

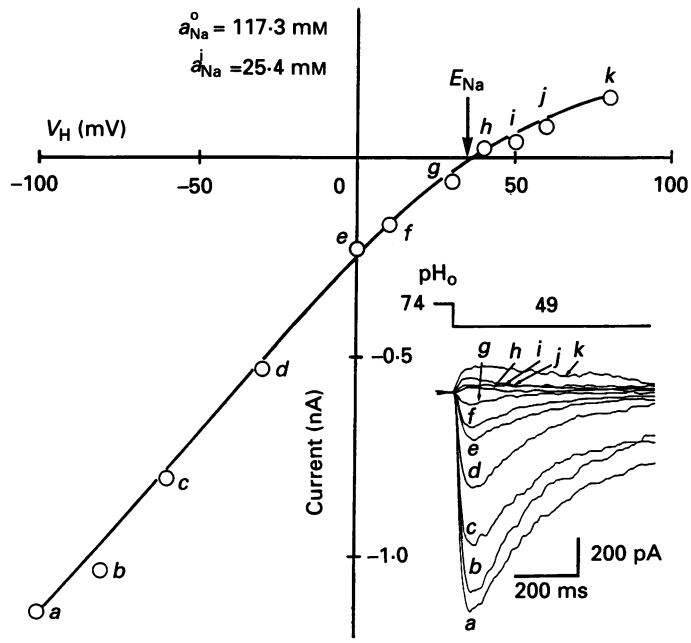

Fig. 8. Voltage dependence of proton-induced current. Neurone was perfused with extracellular and intracellular solutions containing 150 and 30 mM-Na^+, respectively. Superimposed currents shown in inset were induced by a change of pH_o from 7·4 to 4·9 at various V_H. E_{Na} is the Na^+ equilibrium potential.

relationship between a^o_{Na} and E_{proton}. In this figure, the data points were fitted well by a line having a slope of 58 mV/decade for a tenfold change in a^o_{Na} (dashed line), indicating that the proton-induced current behaves like a Na^+ electrode.

To further characterize the ion selectivity of the proton-activated channel, the permeability of other alkali earth metals was examined. Neurones were perfused with the intra- and extracellular solutions containing 6 and 60 mM-Na^+, respectively. After 60 mM-Na^+ in the external solution was replaced with equimolar Li^+, K^+, Rb^+ or Cs^+ the pH_o was decreased from 7·4 to 4·9 and the E_{proton} values in the presence of each cation were measured. The permeability of the channel for these monovalent cations compared to Na^+ was in the order of $Li^+ > Na^+ \gg K^+ > Rb^+ > Cs^+$. The mean selectivity ratio in six cells for each cation was found to be: P_X/P_{Na} = 1·1 ± 0·04, 0·08 ± 0·03, 0·07 ± 0·02, and 0·05 ± 0·03 for Li^+, K^+, Rb^+ and Cs^+, respectively (mean ± S.E.M, n = 4). This order of selectivity fitted that found for the Eisenman series XI; i.e. a strong field strength site (Eisenman, 1962). The order of permeability indicated by the proton-activated channel is the kind of series that is usually associated with the Na^+ channel (Eisenman, 1962).

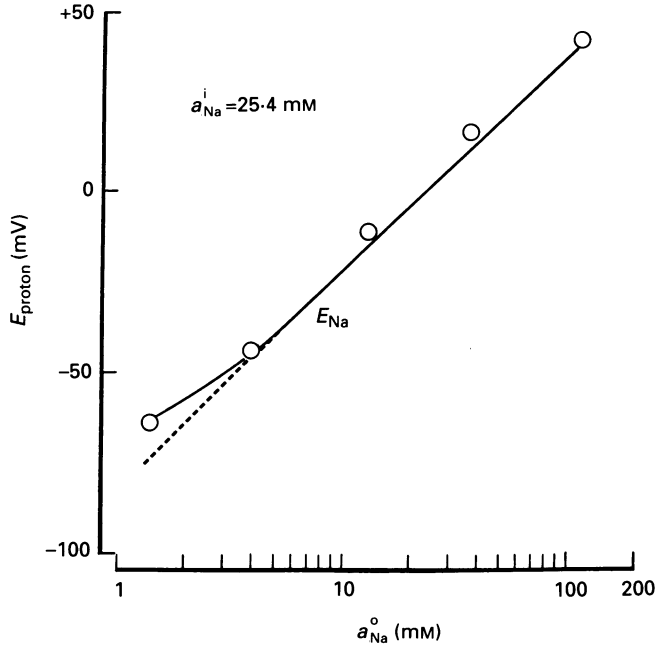

Fig. 9. Correspondence of E_{Na} and E_{proton}. Each point is the mean of four neurones. The $[Na^+]_o$ and $[Na^+]_i$ were 150 and 30 mM, respectively. Abscissa shows active Na^+ concentration (mM). The dashed line represents calculated E_{Na} from the Nernst equation.

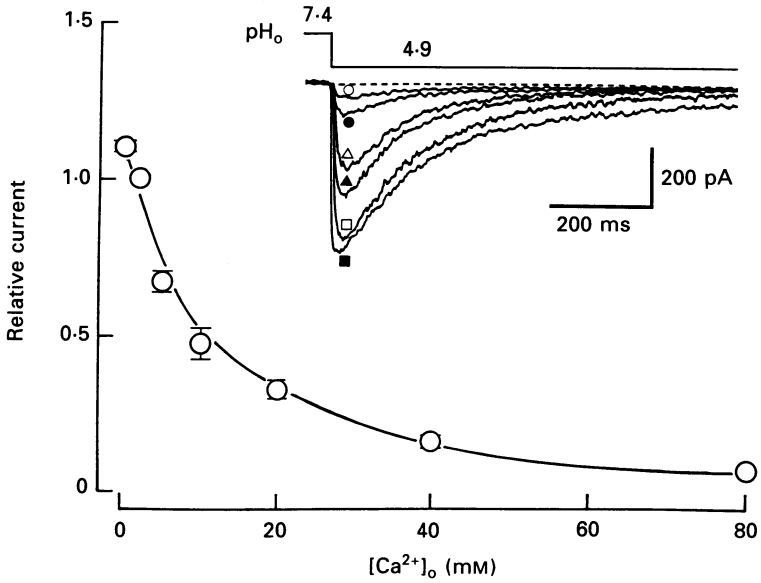

Fig. 10. Effect of $[Ca^{2+}]_o$ on the proton-induced response. Responses were induced by step increase of $[H^+]_o$ from pH_o 7·4 to 4·9 at V_H −80 mV. Each point is the mean of four neurones. Inset shows effect of $[Ca^{2+}]_o$ on amplitude and current kinetics of the proton-induced current: ○ 80, ● 40, △ 10, ▲ 5, □ 2, ■ 0·01 mM $[Ca^{2+}]_o$.

Effect of $[Ca^{2+}]_o$ *on the proton-induced current*

It has already been reported that the proton-induced current in rat sensory neurones has a Ca^{2+} component with $P_{Ca}/P_{Na} = 0{\cdot}31$ (Kovalchuk, Krishtal & Nowycky, 1990). In rat VMH neurones the proton-induced current also had a Ca^{2+}

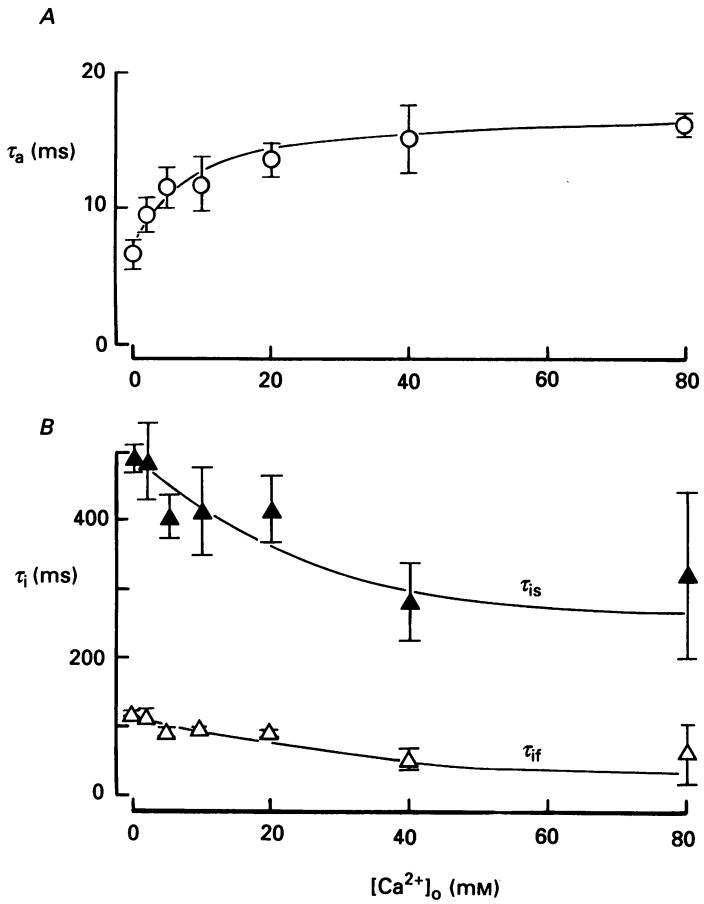

Fig. 11. Effects of $[Ca^{2+}]_o$ on the kinetics of the proton-induced inward current. *A*, relationship between τ_a and $[Ca^{2+}]_o$. Each point is the mean of four neurones. *B*, relationship between τ_{if} or τ_{is} and $[Ca^{2+}]_o$. Each point is the mean of four neurones.

component when external NaCl was replaced by equimolar choline chloride. The Ca^{2+} component in VMH neurones was less than one-tenth of the control current with Na^+. Therefore, we investigated the effect of $[Ca^{2+}]_o$ on the proton-induced current with external solution containing 150 mM-Na^+. All currents were evoked by decreasing pH_o from 7·4 to 4·9. Increasing $[Ca^{2+}]_o$ from Ca^{2+} free (0·01 mM) to 80 mM decreased the peak amplitude of proton-induced current in a concentration-dependent manner (Fig. 10). The kinetics of proton-induced current were also affected with higher $[Ca^{2+}]_o$: increasing $[Ca^{2+}]_o$ increased the τ_a in a hyperbolic manner which finally

saturated between 40 and 80 mM $[Ca^{2+}]_o$, while it slightly decreased both τ_{if} and τ_{is} values (Fig. 11).

Other divalent cations also had an inhibitory effect on the proton-induced current. For these experiments 10 mM $[Ca^{2+}]_o$ was replaced with equimolar Mn^{2+}, Co^{2+}, Sr^{2+},

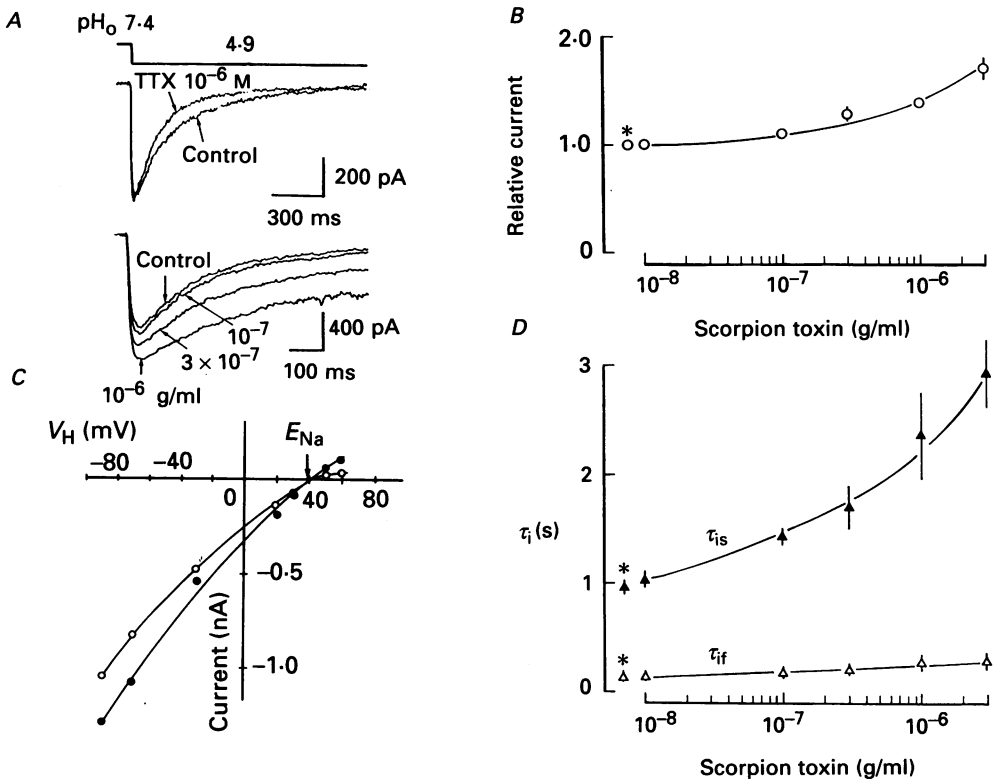

Fig. 12. Effects of tetrodotoxin (TTX) and scorpion toxin on the proton-induced current. *A*, upper panel, effect of TTX (10^{-6} M) on proton-induced current. Lower panel, effect of scorpion toxin at various concentrations (g/ml) on proton-induced current. The pH_o was changed from 7·4 to 4·9. V_H was −80 mV. *B*, effect of scorpion toxin on the peak amplitude of proton-induced current. Each point indicates the mean value of four cells. * is the control value. *C*, *I–V* relationships of proton-induced current elicited by decreasing pH_o from 7·4 to 4·3 at various V_H with (●) or without (○) scorpion toxin (10^{-6} g/ml). Reversal potential of proton-induced currents was not affected by scorpion toxin. *D*, concentration-dependent changes in the fast and slow time constants (τ_{if} and τ_{is}, respectively) in the inactivation phase of proton-induced current. * are control values before applying scorpion toxin. Each point is the mean of four neurones.

Ba^{2+} or Mg^{2+} and then proton-induced currents were elicited by a step decrease in pH_o from 7·4 to 4·3 at a V_H of −80 mV. The peak current amplitudes in the presence of these divalent ions were compared to that in the presence of the calcium ion. The average ratios of the peak currents for other divalent cations were: P_X/P_{Ca} = 0·82±0·05, 0·9±0·04, 1·1±0·2, 1·25±0·07 and 1·31±0·05 for Mn^{2+}, Co^{2+}, Sr^{2+}, Ba^{2+} and Mg^{2+}, respectively (means±S.E.M., $n = 4$). This result indicates that the peak

amplitude of proton-induced currents was inhibited by divalent cations in the order of $Mn^{2+} > Co^{2+} > Ca^{2+} > Sr^{2+} > Ba^{2+} > Mg^{2+}$.

Pharmacological properties of the proton-induced current

Proton-induced currents were elicited by decreasing pH_o from 7·4 to 4·3 at a V_H of −80 mV. TTX (10^{-6} M), a highly specific blocker of the voltage-gated Na^+ channel, did not significantly inhibit the peak amplitude of the proton-induced current in eleven neurones (8·5 ± 4·3 % inhibition $P \leqslant 0{\cdot}001$; mean ± S.E.M., $n = 11$). Usually, TTX (10^{-6} M) had no effect on either the amplitude or the time course of the proton-induced current, although a small increase in the rate of inactivation was noted in three out of eleven neurones studied.

It is well known that scorpion toxin acts on the inactivation phase of voltage-dependent Na^+ current. In our experiments the toxin increased the peak amplitude of the proton-induced current and prolonged its inactivation phase in a concentration-dependent manner (Fig. 12*A* and *B*). Scorpion toxin (10^{-6} g/ml) was effective at various V_H, and it did not shift the reversal potential (Fig. 12*C*). The τ_{is} became larger with higher concentrations of scorpion toxin whereas τ_{if} was not affected (Fig. 12*D*). These effects of the toxin on the proton-induced current did not recover after removing the toxin from the external solution. Such an irreversible effect of scorpion toxin was also observed in the voltage-dependent Na^+ current (I_{Na}) of isolated rat hippocampal neurones (Kaneda, Oyama, Ikemoto & Akaike, 1989*b*). Veratridine has been known to be a lipid-soluble alkaloid and to shift the voltage dependence of activation of I_{Na} to the left. However, this alkaloid (10^{-4} M) had no effect on the proton-induced current in six neurones. The peak amplitude of proton-induced current with 10^{-4} M-veratridine was 97·2 ± 1·2 % (mean ± S.E.M., $n = 6$) of the control.

DISCUSSION

The present study investigated the kinetics of proton-induced current and characterized the ions carrying it. We reported that $[Ca^{2+}]_o$ and $[H^+]_o$ affected the kinetics of proton-induced current in an opposite manner and that the ionic channels for proton-induced current have toxin binding sites similar to those of voltage-dependent Na^+ channels.

Effects of divalent ions on the proton-induced current

Raised $[Ca^{2+}]_o$ inhibited the peak amplitude of proton-induced current while reduced $[Ca^{2+}]_o$ had the opposite effect. Several other divalent ions had similar effects on proton-induced current. The order of divalent ions in inhibiting proton-induced current was similar to that producing voltage shifts in Na^+ channel activation (Hille, Woodhull & Shapiro, 1975). These results suggest that the inhibitory effect of $[Ca^{2+}]_o$ on proton-induced current is responsible for a 'stabilizing' action of Ca^{2+} (Brink, 1954), and that other divalent cations act on proton response as similar stabilizers to Ca^{2+}.

Kinetic properties of proton-induced current

In rat VMH neurones, the activation phase of the proton-induced current followed an exponential time course, with a voltage-independent time constant that decreased with decreasing pH_o. A similar behaviour has been reported for cultured chick DRG neurones (Konnerth *et al.* 1987), dissociated frog DRG neurones (Akaike *et al.* 1990) and parasympathetic neurones dissociated from frog heart (Kim *et al.* 1990) The activation of the current in VMH neurones was slowed when $[Ca^{2+}]_o$ was raised over the range 0·001–80 mM, whereas the activation of the proton-induced current in frog parasympathetic and DRG neurones showed little or no dependence on $[Ca^{2+}]_o$ (Kim *et al.* 1990).

The inactivation of the proton-induced current differed in several ways from the inactivation seen in other cells that have been studied. Two phases of inactivation (τ_{if} and τ_{is}) were seen in VMH neurones while only one phase has been reported for other cell types (Konnerth *et al.* 1987; Akaike *et al.* 1990; Kim *et al.* 1990). The time constants of both components increased slightly with decreasing pH_o over the range pH 5·5–4·1 at which the current was evoked. This is different to the single inactivation component seen in frog parasympathetic and DRG neurones which showed a more rapid inactivation as $pH_o$was lowered between pH 7·0 and 5·5. The difference in behaviour may simply reflect the different pH ranges studied. It is possible that inactivation was slowed at very low pH_o in all cell types but was noted only in VMH neurones which required such pH_o for activation. The acceleration seen with acidification in the other preparations would not be observed in VMH neurones as little or no current was evoked over the pH range 7·0–5·5. Raising $[Ca^{2+}]_o$ caused a slight decrease in both τ_{is} and τ_{if} in VMH neurones. No such Ca^{2+} dependence has been reported for the inactivation of the proton-induced current in other preparations; however, the range of concentrations examined in the current investigation (0·001–80 mM) is far greater than that used in the earlier studies (0·1 up to 2–10 mM; Kim *et al.* 1990). One consistent finding is that the inactivation process appears to be voltage independent in all preparations studied.

In VMH neurones the activation curve was at more acidic values than those of other preparations (Fig. 2*B*). Lower pH_o – less than 4·5 – prolonged the inactivation phase of proton-induced current while the peak amplitudes of currents were slightly increased. Therefore, both τ_{if} and τ_{is} values in VMH neurones increased at lower pH_o. These results suggest that modulation of $[H^+]_o$ on the inactivation phase becomes detectable at lower pH_o. Moreover, the inactivation kinetics of proton response in rat VMH neurones were dependent on $[Ca^{2+}]_o$. Both τ_{if} and τ_{is} were decreased as $[Ca^{2+}]_o$ increased from 0·01 to 80 mM, and the inactivation phase of proton-induced current became slower with lower $[Ca^{2+}]_o$.

Characterization of the proton-activated ionic channel

Tetrodotoxin had no inhibitory effect on the proton-induced Na^+ current in cultured mouse spinal neurones (Gruol, Barker, Huang, MacDonald & Smith, 1980), cultured chick DRG neurones (Konnerth *et al.* 1987), freshly dissociated rat trigeminal neurones (Krishtal & Pidoplichko, 1981*b*) and frog parasympathetic ganglion cells (Kim *et al.* 1990). In VMH neurones, the peak amplitude of the proton-

induced current was also insensitive to TTX at concentrations which completely block the voltage-gated Na^+ current (Kaneda *et al.* 1989*a*). The inactivation phase of proton-induced current, however, was slightly accelerated by TTX, as observed in frog dorsal root ganglion cells (Akaike *et al.* 1990). This suggests that the ionic channels activated by H^+ may have receptive sites for TTX. Scorpion toxin increased the peak amplitude of the proton-induced current and prolonged its inactivation phase. The effect of the toxin on proton-induced current was similar to that on the voltage-dependent Na^+ current of rat hippocampal neurones (Kaneda *et al.* 1989*b*) and rat VMH neurones (N. Akaike & S. Ueno, unpublished observation). These results also suggest that the H^+-activated channels have binding sites for scorpion toxin, similar to those in voltage-dependent Na^+ channels.

Konnerth *et al.* (1987) suggested that the proton-induced Na^+ current flows through a proton-transformed Ca^{2+} channel. This suggestion came from pharmacological experiments in which organic and inorganic Ca^{2+} channel blockers suppressed the proton response (Konnerth *et al.* 1987). However, the effective doses of organic Ca^{2+} channel blockers used by Konnerth and colleagues were extremely high. At high concentrations, these organic Ca^{2+} channel antagonists were non-selective since they suppressed not only the voltage-gated Ca^{2+} channel but also the voltage-gated Na^+ channel in frog neurones (Yakushiji, Tokutomi, Akaike & Carpenter, 1987; Akaike *et al.* 1990; Kim *et al.* 1990). Furthermore, our present experiments indicate that the proton-activated ionic channels may have respective toxin binding sites for both TTX and scorpion toxin. Therefore, the ionic channels that protons modify are very likely to be Na^+ channels. However, in rat VMH neurones and other preparations TTX did not have a significant inhibitory effect on the proton-induced current even at high concentration (more than 10^{-6} M). Na^+ channels are known to become insensitive to TTX when pH_o is lowered (Hille, 1971; Ulbricht & Wagner, 1975) as protons occupy the TTX binding sites with Na^+ channels. The observations suggest that the proton-induced current might flow through a Na^+ channel.

We found that most of rat hippocampal neurones failed to respond to pH_o reduction in spite of the presence of both voltage-dependent Na^+ and Ca^{2+} channels (N. Akaike, S. Ueno & T. Nakaye, unpublished observations). Such proton-insensitive neurones were also reported in 75% of rat spinal and trigeminal ganglion cells having diameters larger than 26 μm (Krishtal & Pidoplichko, 1981*a*), and freshly dissociated frog DRG cells having diameters larger than 20 μm (Akaike *et al.* 1990). In contrast, all of rat dissociated VMH neurones elicited the proton response. Three subtypes of voltage-gated Na^+ channels have been reported in brain tissue (Goldin *et al.* 1986; Noda, Ikeda, Suzuki, Takeshima, Takahashi, Kuno & Numa, 1986) and one or more of these subtypes may be responsible for the proton-induced current. Alternatively, this current may flow not through voltage-gated Na^+ channels but through proton receptor-gated channels.

Possible pathological role of proton-induced current

All proton-activated ionic channels reported previously in chick DRG cells (Konnerth *et al.* 1987), frog DRG cells (Akaike *et al.* 1990) and frog heart parasympathetic ganglion cells (Kim *et al.* 1990) were largely or completely

inactivated around the physiological pH_o range. Thus, the pH_o for half-maximum inactivation was 7·11–7·32 at $[Ca^{2+}]_o$ = 1–5 mM in cultured chick DRG cells (Konnerth *et al.* 1987) and 7·75 at $[Ca^{2+}]_o$ = 2 mM in dissociated frog parasympathetic ganglion cells (Kim *et al.* 1990). Furthermore, they required conditioning pH_o (alkalosis) higher than the physiological range to elicit the proton-induced current in response to reduced pH_o (acidosis). In contrast, the activation and inactivation curves for proton-induced current in VMH neurones was at a more acidic value than those of peripheral neurones, indicating that the ionic channel carrying the proton-induced current in the VMH neurones could be fully activated at a physiological pH_o. Therefore, the proton-induced current may be responsible for certain pathological states such as ischaemia, seizure and trauma, where a reduction in pH_o occurs (Cragg *et al.* 1977; Kraig *et al.* 1983) The steady-state inhibition curve of VMH neurones shows that more than 75% of the ionic channels are still active at pH_o 7·0–6·5 where neuronal excitability is depressed (Hille, 1968; Balestrino & Somjen, 1988; Jarolimek, Misgeld & Lux, 1989) and sodium pump activity is reduced (Akaike & Kiyohara, 1981). Even in such severe conditions, further reduction of pH_o can induce Na^+ current resulting in accumulation of intracellular Na^+. This could be linked to neuronal death in brain ischaemia.

The authors thank Dr N. Agopyan for critical reading of this manuscript. This study was supported by Grants-in-Aid for Scientific Research (nos. 02241101, 02404022 and 02304031) funded to N.A. by the Ministry of Education, Science and Culture, Japan.

REFERENCES

AKAIKE, N., INOUE, M. & KRISHTAL, O. A. (1986). 'Concentration-clamp study' or γ-aminobutyric-acid-induced chloride current kinetics in frog sensory neurones. *Journal of Physiology* **379**, 171–185.

AKAIKE, N. & KIYOHARA, S. (1981). The K^+-sensitive hyperpolarization of rat skeletal muscle and metabolic inhibitors. *Japanese Journal of Physiology* **31**, 169–179.

AKAIKE, N., KOSTYUK, P. G. & OSIPCHUK, Y. V. (1989). Dihydropyridine-sensitive low-threshold calcium channels in isolated rat hypothalamic neurones. *Journal of Physiology* **412**, 181–195.

AKAIKE, N., KRISHTAL, O. A. & MARUYAMA, T. (1990). Proton-induced sodium current in frog isolated dorsal root ganglion cells. *Journal of Neurophysiology* **63**, 805–813.

BALESTRINO, M. & SOMJEN, G. G. (1988). Concentration of carbon dioxide, interstitial pH and synaptic transmission in hippocampal formation of the rat. *Journal of Physiology* **396**, 247–266.

BEGENISICH, T. B. & DANKO, M. (1983). Hydrogen ion block of the sodium pore in squid giant axons. *Journal of General Physiology* **82**, 599–618.

BRINK, F. (1954). The role of calcium ions in neural processes. *Pharmacological Reviews* **6**, 243–298.

CAMPBELL, D. T. (1982). Do protons block Na^+ channels by binding to a site outside the pore? *Nature* **298**, 165–167.

CAMPBELL, D. T. & HILLE, B. (1976). Kinetic and pharmacological properties of the sodium channel of frog skeletal muscle. *Journal of General Physiology* **67**, 309–323.

CRAGG, P., PATTERSON, L. & PURVES, M. J. (1977). The pH of brain extracellular fluid in the cat. *Journal of Physiology* **272**, 137–166.

EISENMAN, G. (1962). Cation selective glass electrodes and their mode of operation. *Biophysical Journal* **2**, suppl. 2, 259–323.

GOLDIN, A., SNUTCH, T., LUBBERT, H., DOWSETT, A., MARSHALL, J., AULD, V., DOWNEY, W., FRITZ, L., LESTER, H., DUNN, R., CATTERALL, W. A. & DAVIDSON, N. (1966). Messenger RNA coding for only the α subunit of the rat brain Na channel is sufficient for expression of functional channels in *Xenopus* oocytes. *Proceedings of the National Academy of Sciences of the USA* **83**, 7503–7507.

GRANTYN, R. & LUX, H. D. (1988). Similarity and mutual exclusion of NMDA- and proton-activated transient Na^+-currents in rat tectal neurons. *Neuroscience Letters* **89**, 198–203.

GRAY, R. & JOHNSTON, D. J. (1985). Rectification of single GABA-gated chloride channels in adult hippocampal neurons. *Neurophysiology* **54**, 134–142.

GRUOL, D. L., BARKER, J. L., HUANG, L. M., MACDONALD, J. F. & SMITH, T. G. JR (1980). Hydrogen ions have multiple effects on the excitability of cultured mammalian neurons. *Brain Research* **183**, 247–252.

HILLE, B. (1968). Charges and potentials at the nerve surface: Divalent ions and pH. *Journal of General Physiology* **51**, 221–236.

HILLE, B. (1971). The permeability of the sodium channel to organic cations in myelinated nerve. *Journal of General Physiology* **58**, 599–619.

HILLE, B., SHAPIRO, B. I. & WOODHULL, A. M. (1975). Negative surface charge near sodium channels of nerve: Divalent ions, monovalent ions, and pH. *Philosophical Transactions of the Royal Society* B **270**, 301–318.

JAROLIMEK, W., MISGELD, U. & LUX, H. D. (1989). Activity dependent alkaline and acid transients in guinea pig hippocampal slices. *Brain Research* **505**, 225–232.

KANEDA, M., OYAMA, Y., IKEMOTO, Y. & AKAIKE, N. (1989*a*). Blockade of the voltage-dependent sodium current in isolated rat hippocampal neurons by tetrodotoxin and lidocaine. *Brain Research* **484**, 348–351.

KANEDA, M., OYAMA, Y., IKEMOTO, Y. & AKAIKE, N. (1989*b*). Scorpion toxin prolongs an inactivation phase of the voltage-dependent sodium current in rat isolated single hippocampal neurons. *Brain Research* **487**, 192–195.

KIM, D. K., TATEISHI, N. & AKAIKE, N. (1990). Proton-gated sodium current in parasympathetic ganglion cells of frog heart. *Journal of Neurophysiology* **63**, 805–813.

KONNERTH, A., LUX, H. D. & MORAD, M. (1987). Proton-induced transformation of calcium channel in chick dorsal root ganglion cells. *Journal of Physiology* **386**, 603–633.

KOVALCHUK, YU. N., KRISHTAL, O. A. & NOWYCKY, M. C. (1990). The proton-activated inward current of rat sensory neurons includes a calcium component. *Neuroscience Letters* **115**, 237–242.

KRAIG, R. P., FERREIRA-FILHO, C. R. & NICHOLSON, C. (1983). Alkaline and acid transients in cerebellar microenvironment. *Journal of Neurophysiology* **49**, 831–850.

KRISHTAL, O. A. & PIDOPLICHKO, V. I. (1981*a*). A receptor for protons in the membrane of sensory neurons may participate in nociception. *Neuroscience* **6**, 2599–2601.

KRISHTAL, O. A. & PIDOPLICHKO, V. I. (1981*b*). A receptor for protons in the nerve cell membrane. *Neuroscience* **5**, 2325–2327.

NAKAGAWA, T., SHIRASAKI, T., TATEISHI, N., MURASE, K. & AKAIKE, N. (1990). Effects of antagonists on *N*-methyl-D-aspartate response in acutely isolated nucleus tractus solitarii neurons of the rat. *Neuroscience Letters* **113**, 169–174.

NODA, M., IKEDA, T., SUZUKI, T., TAKESHIMA, H., TAKAHASHI, T., KUNO, M. & NUMA, S. (1986). Expression of functional sodium channels from cloned cDNA. *Nature* **322**, 826–828.

SHIRASAKI, T., NAKAGAWA, T., WAKAMORI, M., TATEISHI, N., FUKUDA, A., MURASE, K. & AKAIKE, N. (1990). Glycine-insensitive desensitization of *N*-methyl-D-aspartate receptors in acutely isolated mammalian cental neurons. *Neuroscience Letters* **108**, 93–98.

TAKAHASHI, K. & AKAIKE, N. (1990). Nicergoline inhibits T-type Ca^{2+} channels in rat isolated hippocampal CA1 pyramidal neurones. *British Journal of Pharmacology* **100**, 705–710.

TAKAHASHI, Y. & OGAWA, T. (1987). Effects of lowered pH of the extracellular solution on non-transsynaptic component of evoked potentials in the rat's *in vitro* cerebral cortical slices. *Tohoku Journal of Experimental Medicine* **152**, 63–65.

ULBRICHT, W. & WAGNER, H. H. (1975). The influence of pH on equilibrium effects of tetrodotoxin on myelinated nerve fibres of *Rena esculenta*. *Journal of Physiology* **252**, 159–184.

WAKAMORI, M., KANEDA, M., OYAMA, Y. & AKAIKE, N. (1989). Effects of chlorpromazine, diazepam, diphenylhydantoin, flunitrazepam and haloperidol on the voltage-dependent sodium current of isolated mammalian brain neurons. *Brain Research* **494**, 374–378.

YAKUSHIJI, T., TOKUTOMI, N., AKAIKE, N. & CARPENTER, D. O. (1987). Antagonists of GABA responses, studied using internally perfused frog dorsal root ganglion neurones. *Neuroscience* **22**, 1123–1133.